Unstable hadrons in hot hadron gas: In the laboratory and in the early Universe

Inga Kuznetsova* and Johann Rafelski
Department of Physics, University of Arizona, Tucson, Arizona, 85721, USA
(Received 2 February 2010; published 9 September 2010)

We study kinetic master equations for chemical reactions involving the formation and the natural decay of unstable particles in a thermal bath. We consider the decay channel of one into two particles and the inverse process, fusion of two thermal particles into one. We present the master equations for the evolution of the density of the unstable particles in the early Universe. We obtain the thermal invariant reaction rate using as an input the free space (vacuum) decay time and show the medium quantum effects on $\pi+\pi \leftrightarrow \rho$ reaction relaxation time. As another laboratory example we describe the $K+K \leftrightarrow \phi$ process in thermal hadronic gas in heavy-ion collisions. A particularly interesting application of our formalism is the $\pi^0 \leftrightarrow \gamma+\gamma$ process in the early Universe. We also explore the physics of $\pi^\pm$ and $\mu^\pm$ freeze-out in the Universe.

DOI: 10.1103/PhysRevC.82.035203 PACS number(s): 95.30.Cq, 52.27.Ny, 24.10.Pa

I. OVERVIEW

A. Particles in the Universe for $T > 5$ MeV

This study began with the question: At what temperature in the expanding early Universe does the reaction

$$\pi^0 \leftrightarrow \gamma+\gamma \tag{1}$$

"freeze" out, that is, the π^0 decay overwhelms the production rate and the yield falls away from chemical equilibrium yield. Because the π^0 life span (8.4×10^{-17} s) is rather short, one is tempted to presume that the decay process [rightward arrow in Eq. (1)] dominates. However, there must be a detailed balance in the thermal bath: the production process (leftward arrow) in a suitable environment must be able to form π^0 with a strength corresponding to the decay process life span.

We demonstrate here that the π^0 production and equilibration relaxation time is of the same order of magnitude as the life span of π^0 in the post–quark-gluon-plasma (QGP) hadronization Universe, $T < 200$ MeV. The point is that the π^0 life span is much shorter than the Universe expansion time (inverse expansion rate) $1/H$ [2]:

$$H=\frac{\dot R}{R}=1.66\sqrt{g^*}\frac{T^2}{m_{\rm pl}}, \tag{2}$$

where g^* is the number of degrees of freedom. $m_{\rm pl}=1.2211\times10^{19}$ GeV is the Plank mass. Figure 1 compares the π^0 production-equilibration time [solid (blue) line] with the Universe expansion time $1/H$ [dashed (green) line]. We see that the π^0 equilibration time is much shorter, by 14 orders of magnitude at $T=10$ MeV, compared to the Universe expansion time constant.

The reason for this is that in thermal equilibrium the photon density remains high [dash-dotted (red) line in Fig. 2] also for relatively small T. Thus there is a small, non-negligible probability of finding high-energy photons capable of producing π^0, whose density at low T is very small [solid (blue) line in Fig. 2]. The π^0 production has enough time to equilibrate with the decay process. Therefore the π^0 density does not freeze out but decreases with decreasing ambient temperature of the expanding Universe, all the time remaining in chemical equilibrium with the photon abundance.

Let us recall how the Bose distribution describes π^0 density:

$$n^{\rm eq}_{\pi^0}=\int\frac{d^3p}{(2\pi)^3}\frac{1}{e^{u\cdot p/kT}-1}. \tag{3}$$

Here u^μ is the four-velocity of the observer with reference to the heat-bath rest frame, and p^μ is the momentum four-vector,

$$p^\mu=\left(\frac{E}{c},\vec p\right),\quad E=\sqrt{\vec p^{\,2}+m^2}, \tag{4}$$

of the particle considered: a similar expression applies for photons, which have twofold spin degeneracy, and $m\to0$. The resulting π^0 density falls exponentially when $kT < m_{\pi^0}c^2$ (henceforth units are chosen such that $\hbar=c=k=1$). However, this density remains high compared to the nucleon's density in the Universe (dotted (black) line in Fig. 2; taken from Ref. [4]), down to a temperature of about 6 MeV. This is the lower T limit of validity in our present study, as we consider particle production reactions in a particle-antiparticle-symmetric Universe.

Some of the results we derive here were presented in [3] without a derivation: there we considered a laboratory $e^+e^-\gamma$ plasma and postponed the theoretical and analytical details. Here we evaluate the reaction relaxation time for reactions involving two particles fusing into one particle and/or particle decay into two, Eq. (1), and relate this to the life span of decaying particles in vacuum. To complement this, in Sec. IV C we also consider $\pi^\pm$, which can be equilibrated by the reaction

$$\pi^0+\pi^0 \leftrightarrow \pi^+ +\pi^- \tag{5}$$

and, also, by reactions involving muons,

$$\pi^\pm \leftrightarrow \mu^\pm+\nu_\mu(\bar\nu_\mu). \tag{6}$$

We also consider how rapidly muons are produced in the reactions

$$\gamma+\gamma \leftrightarrow \mu^+ +\mu^-,\quad e^+ +e^- \leftrightarrow \mu^+ +\mu^- \tag{7}$$

*ikouznet@email.arizona.edu

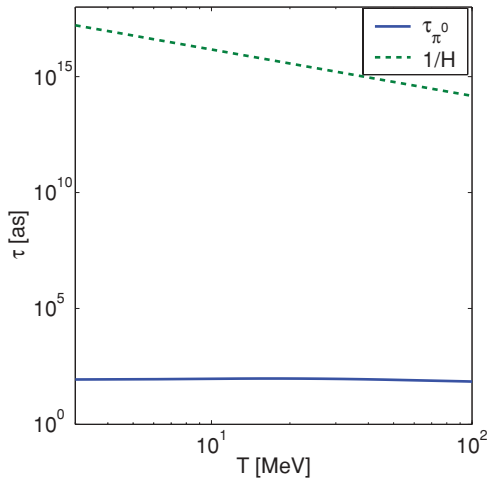

FIG. 1. (Color online) π^0 equilibration time [solid (blue) line] and Universe expansion time $1/H$ as functions of temperature [dashed (green) line].

and show that these particles also do not freeze out down to a T value of a few mega–electron volts [3]. The muon density is slightly higher than that pions because of their smaller mass; see the dashed (green) line in Fig. 2. Another reaction that may influence muon chemical equilibration is the decay of one particle to three particles and the reverse reaction, including neutrinos:

$$\mu^{\pm} \leftrightarrow e^{\pm} + \nu_e(\bar{\nu}_e) + \bar{\nu}_\mu(\nu_\mu). \tag{8}$$

However, in this case the exact influence of medium effects on the reaction rate is more complicated and we do not consider this reaction in complete detail here. We do, however, compare the relaxation times of particle production in all mentioned reactions with the Universe expansion rate to see if the particle densities stay in chemical equilibrium.

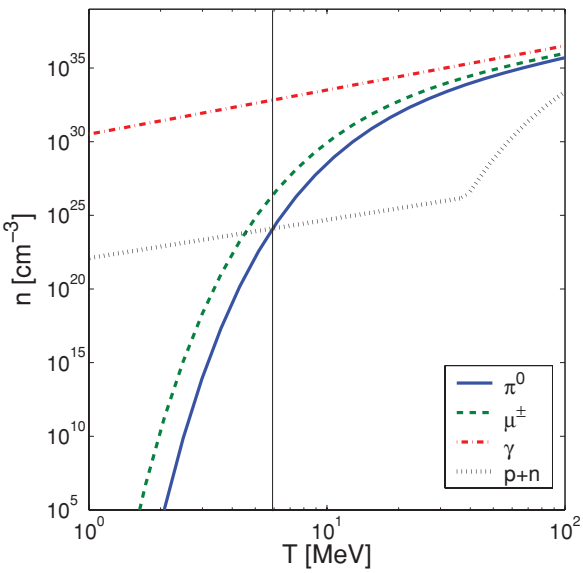

FIG. 2. (Color online) Thermal equilibrium density as a function of temperature for γ [dash-dotted (red) line], π^0 [solid (blue) line], $\mu^{\pm}$ pair [dashed (green) line], and nucleons $p+n$ [dotted (black) line] [4].

B. Degrees of freedom in the Universe

The life spans of all unstable hadrons and leptons, except for neutrons n, are much shorter than the Universe expansion rate for $5 < T < 200$ MeV. Here we show that, as a result, all unstable particles stay in chemical equilibrium, including neutrons which are effectively stable on the time scale of expansion. The importance of this remark is that we can evaluate the active effective degeneracy (degrees of freedom) in the Universe in the entire temperature domain including all unstable hadron states. In the hadron phase we define the effective degeneracy using as reference the Stephan-Boltzmann law,

$$g_E(T) = \frac{\epsilon}{\sigma T^4}, \quad \sigma = \frac{\pi^2}{30}, \tag{9}$$

where ϵ is the energy density,

$$\epsilon = \int \sum_i g_i E_i f_i(p)\, d^3p, \quad E_i = \sqrt{m_i^2 + \vec{p}^{\,2}}, \tag{10}$$

with the sum over all particles present.

In Fig. 3 we show the degeneracy, Eq. (9), as a function of T. The dashed (red) line accounts for the photon, three families of neutrino and antineutrino, electron, positron, muon, and antimuon contributions. The dot-dashed (green) line adds pions; the solid (blue) line, all hadrons. Pions begin to contribute noticeably to degeneracy at $T > 30$ MeV. Among hadrons we included all light and strange mesons and baryons, up to a mass of about 1700 MeV. The finite density of p and n is also included. As noted earlier, this is a more complicated case; fortunately the finite baryon density contributes, at most, just a few percent to g_E near the hadronization temperature, where the particle-antiparticle symmetry is good to 10 orders of magnitude.

The boundary between quark-gluon and hadron phase (vertical line) is near $T_h = 170$ MeV. In Fig. 3 we also

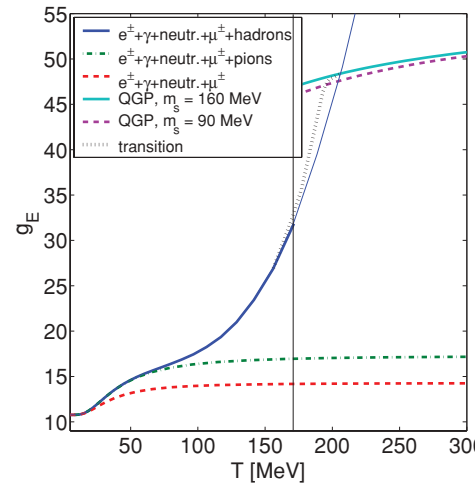

FIG. 3. (Color online) Effective degeneracy g_E in the Universe based on the energy density of hadrons and for QGP, as a function of T. See text for more details.

show degeneracy in QGP for $T > 160$ MeV (upper lines). The results shown are based on our earlier detailed study of QGP properties [8]. Here the QGP degeneracy is shown for the extreme case of either strange quark $m_s = 90$ MeV [upper dashed (purple) line] or strange quark $m_s = 160$ MeV [upper solid (turquoise) line]. Because the expansion of the Universe is relatively slow compared to the expansion of QGP in the laboratory, heavy and strange quarks also have enough time to reach chemical equilibrium density in the QGP temperature range presented in Fig. 3.

Figure 3 shows that the effective degeneracy of hadrons, while rising fast, is still smaller than the degeneracy in QGP in the domain of phase transformation temperature near 160–170 MeV. Many heavy hadron states may be missing from the experimental tables. Even though their individual contribution to the degeneracy is decreasing, their number is expected to grow rapidly, in accordance with the Hagedorn hypothesis, in which the hadron mass spectrum diverges exponentially near the hadronization temperature. This theoretical exponentially growing component leads to a smoother transition between hadronic gas and QGP, as is qualitatively indicated in Fig. 3 [dotted (black) line].

C. Production and decay of unstable particles

We show here for the first time the detailed derivation of relaxation time for reactions involving one to two particles in the thermal medium, which we considered in Refs. [6–8]. In the rest frame of the decaying particle m_3, the reaction

$$A_1 + B_2 \leftrightarrow C_3 \tag{11}$$

requires that $m_1 + m_2 \leqslant m_3$, which allows the spontaneous decay process. This is easily seen considering

$$\begin{aligned} m_3^2 &= (p_1 + p_2)^2 \\ &= (m_1 + m_2)^2 + 2(E_1E_2 - m_1m_2 - \vec{p}_1 \cdot \vec{p}_2) \\ &\geqslant (m_1 + m_2)^2. \end{aligned} \tag{12}$$

In the last inequality we used $E_1^2E_2^2 \geqslant (m_1m_2 + \vec{p}_1 \cdot \vec{p}_2)^2$, which can be reorganized to read $(m_1\vec{p}_2 - m_2\vec{p}_1)^2 \geqslant \vec{p}_1 \cdot \vec{p}_2 - \vec{p}_1^2\vec{p}_2^2$. This is always true, as the right-hand side is always negative, or 0 if both vectors are parallel. The equality sign corresponds to the case $m_1 + m_2 = m_3$, where the reaction rate vanishes by virtue of vanishing phase space. This textbook exercise shows that the reaction Eq. (1) is possible when condition Eq. (12) is satisfied.

The constraint Eq. (12) forbids many reactions. For example, the hydrogen formation $p + e \to \mathrm{H}$ is forbidden as, for a bound state, $m_H < m_p + m_e$. Thus there must be a second particle in the final state. The electron capture involves either a radiative emission, $p + e \to \mathrm{H} + \gamma$, or a surface/third atom, which picks the recoil momentum. The situation would be different if there were "resonant" intermediate states of relatively long life spans with energies above the ionization threshold. Such "doorway" resonances are available in many important physical processes.

It is natural to evaluate the rates of the processes of interest, Eq. (11), in the rest frame of particle 3, boosting, as appropriate, from or to the laboratory frame. To do this effectively we need the master population equations in an explicitly covariant fashion, which is discussed in Sec. II; see Ref. [6]. The kinetic equation for time evolution of number N of decaying particles 3 can be written as

$$\frac{1}{V}\frac{dN_3}{dt} = \left(\frac{\Upsilon_1\Upsilon_2}{\Upsilon_3} - 1\right)\frac{dW_{3\to 12}}{dVdt}, \tag{13}$$

where $dW_{3\to 12}/dVdt$ is the decay rate of particle 3 and Υ_i is the fugacity of particle i. Here the number density n_i of particle i in thermal (kinetic), but not necessarily in chemical, equilibrium is given by

$$\frac{N_i}{V} \equiv n_i = \frac{1}{(2\pi)^3}\int d^3p_i\, f_{b/f}(p_i), \tag{14}$$

$$f_{b/f}(\Upsilon_i, p_i) = \frac{1}{\Upsilon_i^{-1}e^{(u\cdot p_i - \mu_i)/T} \mp 1}. \tag{15}$$

f is the covariant form of the usual Bose or Fermi distribution function defined in the rest frame of the thermal bath and describes the corresponding quantity in a general reference frame where the thermal bath has the relative velocity defined by u^μ. In the rest frame of the thermal bath frame we have

$$u^\mu \to (1, \vec{0}). \tag{16}$$

p_i is the four-momentum vector of particle i:

$$p_i^\mu = (E_i, \vec{p}_i). \tag{17}$$

μ_i is the chemical potential, which shows the asymmetry in particle and antiparticle densities $\mu_i = -\bar{\mu}_i$. For reactions considered here we have $\mu_i \simeq 0$. This was assumed in Eq. (13). Note that the distribution function f is a Lorentz scalar but the spatial density n_i is not.

Particle C_3 attains the chemical equilibrium when the following condition among fugacities is satisfied:

$$\Upsilon_1\Upsilon_2 = \Upsilon_3. \tag{18}$$

This, as expected, is equivalent to the Gibbs condition for the chemical equilibrium. In Sec. III we evaluate the invariant rate using the vacuum decay time established in the rest frame of the decaying particle, and we discuss the behavior of the average decay rate of an unstable particle in the presence of the thermal bath. In Sec. IV, we apply our formalism to two examples.

(i) We study the formation and decay rate of the ρ meson through $\pi + \pi \leftrightarrow \rho$ in a baryon-free hot hadronic gas, where mesons are considered in thermal and chemical equilibrium.

(ii) We consider the reaction $\gamma + \gamma \leftrightarrow \pi^0$ in the early Universe and find that the expansion of the Universe is slow compared to pion equilibration, which somewhat surprisingly (for us) implies that π^0 is at all times in chemical equilibrium (but at sufficiently low temperatures, e.g., 3–4 MeV, the local density of π^0 is too low to apply the methods of statistical physics).

(iii) We consider the reaction Eq. (6) as an example of the decay of $\pi^\pm$ to fermions, and the reverse reaction, and show that $\pi^\pm$ and $\mu^\pm$ are also in chemical equilibrium until their equilibrium density vanishes at

low temperatures (about 3–4 MeV) because of the large mass. Also, we discuss neutrino equilibration by way of this reaction.

(iv) We study ϕ meson evolution considering the reaction $K + K \leftrightarrow \phi$ in thermal hadronic gas in heavy-ion collisions.

To conclude this overview we draw attention to the fact that, unlike the one-to-two reaction, the two-to-two reactions,

$$A_1 + B_2 \leftrightarrow C_3 + D_4, \tag{19}$$

have been extensively studied in the past, in the context of astrophysics and cosmology [1,2] and heavy-ion reactions [5]. However, the simpler one-to-two situation has escaped attention so far, and the adaptation of kinetic methods is in detail not trivial, given the novel quantum and relativistic effects involving particle decay. Aside from cosmology implications, the insights gained in this study are clearly of relevance to the general understanding of QGP and hadron gas evolution in relativistic heavy-ion collisions. For example, our present work allows to consider the chemical yields arising in reactions such as $\rho \leftrightarrow \pi\pi$, $\pi^0 \leftrightarrow \gamma\gamma$, $\Delta \leftrightarrow N\pi$, and $K + K \leftrightarrow \phi$ [6,7].

II. KINETIC EQUATIONS FOR DECAYING PARTICLES

A. Decaying particle density evolution equation

Consider an unstable particle, say C_3, which decays into other two particles,

$$C_3 \to A_1 + B_2 \tag{20}$$

in the vacuum. In a dense and high-temperature thermal ambient phase, particles A_1 and B_2 are present, and the inverse reaction,

$$A_1 + B_2 \to C_3, \tag{21}$$

can occur, producing the particle we called C_3. For now we assume that the abundance of particle C_3 changes solely by the decay, Eq. (20), and (thermal) production, Eq. (21), reactions. The time variation of the number of particles N_3 then is controlled by the master equation

$$\frac{1}{V}\frac{dN_3}{dt} = \frac{dW_{12\to 3}}{dVdt} - \frac{dW_{3\to 12}}{dVdt}, \tag{22}$$

where $dW_{12\to 3}/dVdt$ is the production rate per unit volume of particle type C_3 via Eq. (21) and $dW_{3\to 12}/dVdt$ is the decay rate of particle type C_3 per unit volume.

A very similar master equation controls the abundance of particles A_1 and B_2:

$$\frac{1}{V}\frac{dN_{1,2}}{dt} = \frac{dW_{3\to 12}}{dVdt} - \frac{dW_{12\to 3}}{dVdt} + R_{\text{other}}, \tag{23}$$

where the rate R_{other} is caused by other reactions influencing the abundance of particles of types A_1 and B_2.

As an example, consider the reaction $\rho \leftrightarrow \pi\pi$ in dense hot matter formed in heavy-ion collisions. Pions can be easily created by inelastic collisions of other hadrons and thus we have to deal with a multicomponent system involving R_{other} when looking at π abundance, but to evaluate ρ abundance the dominant terms are as in Eq. (22). We often can assume that R_{other} dominates the yield gains and losses, and thus we can use the thermal distribution for particles A_1 and B_2, which, in the preceding example, are pions.

In the following, we thus assume that particles A_1 and B_2 are in thermal equilibrium, and further, we assume that the system is spatially homogeneous. In thermal equilibrium, the dynamical information can be obtained from the single-particle distribution function $f(p)$ for each particle; see Eq. (15). f is controlled by two parameters: the temperature T and the fugacity Υ. In this paper, we assume that the fugacity Υ changes over time by way of chemical reactions much more rapidly than does the temperature T of the ambient thermal bath, and thus we can consider reactions at a given constant T. This assumption is certainly valid in the domain of temperatures we consider and may fail only at the very highest primordial T in the early Universe.

B. Decay and production rates

The thermal production rate $dW_{12\to 3}/dVdt$ and the decay rate of particle 3 under the thermal background $dW_{3\to 12}/dVdt$ can then be expressed using these distribution functions for each of the particles involved in the reaction. According to the boson or fermion nature of particle A_1, we have to consider different cases. If particle A_1 is a boson, then there are two cases of the decay and production mode, and if the particle C_3 is a fermion, it can only decay into a boson and a fermion:

$$\text{boson}_3 \longleftrightarrow \text{boson}_1 + \text{boson}_2, \tag{24}$$

$$\text{boson}_3 \longleftrightarrow \text{fermion}_1 + \overline{\text{fermion}_2}, \tag{25}$$

$$\text{fermion}_3 \longleftrightarrow \text{boson}_1 + \text{fermion}_2. \tag{26}$$

Accordingly, the Lorentz invariant transition probability per unit time and unit volume corresponding to the process, Eq. (11), is

$$\begin{aligned}\frac{dW_{12\to 3}}{dVdt} = {} & \frac{1}{1+I}\frac{g_1}{(2\pi)^3}\int\frac{d^3p_1}{2E_1} f_{b,f}(\Upsilon_1, p_1)\frac{g_2}{(2\pi)^3} \\ & \times \int\frac{d^3p_2}{2E_2} f_{b,f}(\Upsilon_2, p_2)\int\frac{d^3p_3}{2E_3(2\pi)^3} \\ & \times (2\pi)^4\delta^4(p_1 + p_2 - p_3)\frac{1}{g_1 g_2} \\ & \times \sum_{\text{spin}} |\langle p_1 p_2|M|p_3\rangle|^2[1 \pm f_{b,f}(\Upsilon_3, p_3)],\end{aligned} \tag{27}$$

where $I = 1$ for the case of a reaction between two indistinguishable particles A_1 and B_2, and $I = 0$ if A_1 and B_2 are distinguishable. The factor $1/(g_1 g_2)$ and the summation are caused by averaging over all initial (iso)spin state. The last factor in Eq. (27) accounts for the enhancement or hindrance of the final-state phase owing to the quantum statistical effect, as introduced first by Uehling and Uhlenbeck [9]. The upper sign, $+$, is for the case when particle C_3 is a boson; the lower sign, $-$, for that when it is a fermion. Equation (27)

is manifestly Lorentz invariant and therefore it can be used in any frame of reference.

This rate is related by a detailed balance relation [6] to the particle C_3 decay rate:

$$\frac{dW_{12\to 3}}{dVdt}\Upsilon_3 = \frac{dW_{3\to 12}}{dVdt}\Upsilon_1\Upsilon_2. \tag{28}$$

Therefore chemical equilibrium $\Upsilon_1\Upsilon_2 = \Upsilon_3$ corresponds to the condition of equal decay and production rates, as we expected. Using Eq. (28), Eq. (22) can be written in the form of Eq. (13).

Equation (13) can be further simplified by defining the decay time in matter of particle i:

$$\tau_i = \frac{dn_i/d\Upsilon_i}{R}, \tag{29}$$

where rate

$$R = \frac{1}{\Upsilon_3}\frac{dW_{3\to 12}}{dVdt} = \frac{1}{\Upsilon_1\Upsilon_2}\frac{dW_{12\to 3}}{dVdt}. \tag{30}$$

We show in the next section that this definition has the right vacuum limit and that the dynamical equations assume a particularly simple form. However, the reader should observe that other definitions could be considered.

It is convenient to introduce kinematic reaction times in analogy to the dynamic expression, Eq. (29). Doing this we cast Eq. (13) into the form of an equation for Υ_3,

$$\dot{\Upsilon}_3 = \frac{1}{\tau_T}\Upsilon_3 + \frac{1}{\tau_S}\Upsilon_3 + \frac{1}{\tau_3}(\Upsilon_1\Upsilon_2 - \Upsilon_3), \tag{31}$$

where we define the kinematic relaxation times related to the evolution of temperature and entropy:

$$\frac{1}{\tau_T} \equiv -T^3 g^* \frac{d(n_\pi/(\Upsilon_3 g^* T^3))/dT}{dn_\pi/d\Upsilon_3}\dot{T}, \tag{32}$$

$$\frac{1}{\tau_S} \equiv -\frac{n_\pi/\Upsilon_3}{dn_\pi/d\Upsilon_3}\frac{d\ln(g^* VT^3)}{dT}\dot{T}. \tag{33}$$

We introduced the minus sign previously in order to have τ_T, $\tau_S > 0$. Compared to our earlier definition [6], we now include g^* in τ_T and τ_S.

While in principle the values of τ_T and τ_S are unrelated, for a given kinematic stage of system evolution the temperature change can be related to entropy change. For example, for the radiation-dominated epoch of the Universe we have

$$\frac{\dot{T}}{T} = -\frac{\dot{R}}{R}. \tag{34}$$

In the radiation-dominated Universe the entropy conservation further implies that

$$\frac{1}{\tau_S} \to 0. \tag{35}$$

Freeze-out from chemical equilibrium arises for

$$\tau_T \approx \tau_3. \tag{36}$$

When τ_T is smaller than τ_3, that is, the kinematic term in Eq. (31) is important, Υ_3 begins to increase, often rapidly, as the number of particles 3 is preserved but their density decreases owing to dilution in expansion. Because $\Upsilon_3 > 1$ the multiplicity of particle 3 in the slow decay is dominant, especially so when the particle 1 and 2 yields remain in chemical equilibrium by the action of other processes. These considerations can be of great importance in the study of dark-matter particle abundance, where the life span against decay and/or annihilation is comparable to the life span of the Universe. We postpone further discussion to a more appropriate opportunity.

III. EVALUATION OF THE INVARIANT DECAY (PRODUCTION) RATE

A. General case

The vacuum decay width of particle C_3 in its own rest frame can be found in textbooks. In our notation,

$$\begin{aligned}\frac{1}{\tau_0} &= \frac{1}{2m_3}\frac{1}{1+I}\int\frac{d^3p_1}{2E_1(2\pi)^3}\int\frac{d^3p_2}{2E_2(2\pi)^3}(2\pi)^4 \\ &\quad\times\delta^4(p_1+p_2-p_3)\frac{1}{g_3}\sum_{\text{spin}}|\langle p_1p_2|M|p_3\rangle|^2 \\ &= \frac{1}{2m_3g_3}\frac{1}{4(I+1)(2\pi)^2}\int\frac{d^3p}{E_1E_2}\delta(E_1+E_2-m_3) \\ &\quad\times\sum_{\text{spin}}|\langle\vec{p},-\vec{p}|M|m_3\rangle|^2 \\ &= \frac{1}{8m_3^2g_3}\frac{p}{(I+1)\pi}\sum_{\text{spin}}|\langle\vec{p},-\vec{p}|M|m_3\rangle|^2.\end{aligned} \tag{37}$$

Here $p = p_1 = p_2$ and $E_{1,2} = \sqrt{p^2+m_{1,2}^2}$ are, respectively, the magnitudes of the momentum and the energies of the two particles A_1 and B_2 in the rest frame of particle C_3:

$$\begin{aligned}E_{1,2} &= \frac{m_3^2 \pm (m_1^2 - m_2^2)}{2m_3}, \\ \vec{p}^{\,2} &= \frac{m_3^2}{4} - \frac{m_1^2+m_2^2}{2} + \frac{(m_1^2-m_2^2)^2}{4m_3^2}.\end{aligned} \tag{38}$$

The magnitude of three-momentum $|\vec{p}|$ is of course the same for particles A_1 and B_2 in the rest frame of decaying particle C_3.

We denote by τ_3' the decay rate of particle C_3 in the rest frame of the thermal bath in which it is emerged, E_3 and p_3 are the corresponding energy and the momentum of particle C_3, which changes with thermal velocity distribution. The thermal decay reaction rate per unit volume $dW_{3\to 1+2}/dVdt$ is then obtained by weighting $1/\tau_3'$ with the probability to find the particle at a given momentum and introducing the Lorentz factor γ, so that $E_3\tau_3'/m_3$ is the decay time of particle 3 with moment p_3:

$$\frac{dW_{3\to 1+2}}{dVdt} = \frac{g_3}{(2\pi)^3}\int d^3p_3 f_{b,f}(\Upsilon_3, p_3)\frac{m_3}{E_3}\frac{1}{\tau_3'}. \tag{39}$$

Comparing Eq. (39) with Eq. (27), we conclude that in medium, at finite temperature T, the decay rate τ_3' of particle

C_3 in the rest frame of the heat bath is given by

$$\frac{1}{\tau_3'} = \frac{1}{2m_3}\frac{1}{1+I}\int \frac{d^3p_1}{2E_1(2\pi)^3}\int \frac{d^2p_2}{2E_2(2\pi)^3}(2\pi)^4 \times \delta^4(p_1+p_2-p_3)\frac{1}{g_3}\sum_{\text{spin}}|\langle p_1p_2|M|p_3\rangle|^2 f_{b,f}(\Upsilon_1, p_1) \times f_{b,f}(\Upsilon_2, p_2)\Upsilon_1^{-1}\Upsilon_2^{-1}\exp(u\cdot p_3/T), \quad (40)$$

which is a Lorentz invariant form, but $u\cdot p_3 \to E_3$, the energy of particle 3 in the rest frame of the thermal bath.

Using the in-vacuum particle C_3 rest-frame decay time, Eq. (37), we find that Eq. (40) takes the form

$$\frac{1}{\tau_3'} = \frac{1}{\tau_0}\frac{e^{E_3/T}}{2}\Phi(p_3). \quad (41)$$

The function $\Phi(p_3)$ is

$$\Phi(p_3) = \int_{-1}^{1} d\zeta \frac{\Upsilon_1^{-1}}{\Upsilon_1^{-1}e^{(a_1-b\zeta)}\pm 1}\frac{\Upsilon_2^{-1}}{\Upsilon_2^{-1}e^{(a_2+b\zeta)}\pm 1}, \quad (42)$$

with

$$a_1 = \frac{E_1E_3}{m_3T}, \quad a_2 = \frac{E_2E_3}{m_3T}, \quad b = \frac{pp_3}{m_3T}, \quad \zeta = \cos\theta = \cos(\vec{p}_2\wedge\vec{p}_1). \quad (43)$$

With this the particle C_3 decay rate per unit volume in a thermally equilibrated system is given by

$$\frac{dW_{3\to 1+2}}{dVdt} = \frac{g_3}{(2\pi^2)}\frac{m_3}{\tau_0}\int_0^\infty \frac{p_3^2dp_3}{E_3}\frac{e^{E_3/T}}{\Upsilon_3^{-1}e^{E_3/T}\pm 1}\Phi(p_3). \quad (44)$$

We were able to evaluate the integral $\Phi(p_3)$ analytically in the absence of particle-antiparticle asymmetry (absence of chemical potentials),

$$\Phi(p_3) = \frac{1}{b(e^{a_1+a_2}\pm\Upsilon_1\Upsilon_2)}\ln\frac{(\Upsilon_2e^{-a_2}\pm e^b)(e^{a_1}\pm\Upsilon_1e^{-b})}{(\Upsilon_2e^{-a_2}\pm e^{-b})(e^{a_1}\pm\Upsilon_1e^{b})}, \quad (45)$$

and in the nonrelativistic limit ($m_3 \gg T, p_3$), this quantity tends to

$$\Phi(p_3\to 0) = 2\frac{\Upsilon_1^{-1}\Upsilon_2^{-1}}{\left(\Upsilon_1^{-1}e^{E_1/T}\pm 1\right)\left(\Upsilon_2^{-1}e^{E_2/T}\pm 1\right)}. \quad (46)$$

B. Decay and production rates in the Boltzmann limit

A useful check of the more complex quantum decay case is the Boltzmann limit. We can then omit unity in the distribution, Eq. (15). This is possible when

$$\Upsilon_i^{-1}e^{u\cdot p_i/T} \gg 1, \quad (47)$$

that is, when $\Upsilon_i \ll 1$ or $T \ll m_3/2$. The condition $T \ll m_3/2$ comes from the fact that the minimal energy of lighter particles is $m_3/2$ in the particle 3 rest frame. In this limit the decay time in the particle 3 rest frame from Eq. (40) $\tau' \to \tau_0$, so that from Eq. (29) we have, for the average decay rate τ in the reference

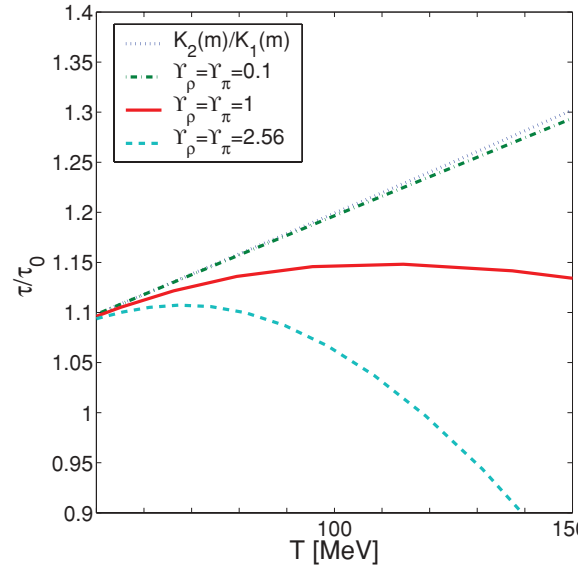

FIG. 4. (Color online) The ratio τ/τ_0 as a function of temperature T in the reaction $\rho \leftrightarrow \pi\pi$. The dotted (blu)e line is for the Boltzmann limit showing only time dilation. Near this limit [dash-dotted (green) line] the dilute system $\Upsilon_\rho = \Upsilon_\pi = 0.1$. Solid (red) line and dashed (turquoise) lines represent $\Upsilon_\rho = \Upsilon_\pi = 1$ and $\Upsilon_\rho = \Upsilon_\pi = 2.56$, respectively.

frame (the rest frame of the bath),

$$\tau_3' \approx \tau_0\frac{\int_0^\infty p^2dp\,e^{E_3/T}}{\int_0^\infty p^2dp\,e^{E_3/T}m_3/E_3} \quad (48)$$

$$= \tau_0\frac{K_2(m_1/T)}{K_1(m_1/T)}. \quad (49)$$

Equation (39) shows that the average decay time τ_3' in the laboratory frame is proportional to the (inverse) average of the Lorentz factor of particle C_3. We address this effect next in a quantitative manner; the ratio of τ_3' to τ_0 is shown in Fig. 4 as the dotted line. For $T \ll m_3$ this ratio goes to unity because the Lorentz factor becomes 1. For large T, the rate increases because of the higher average energy of particle C_3, that is, the increasing average Lorentz factor γ. Therefore, for the low-density classical limit with $\Upsilon_i \ll 1$, the average particle lifetime increases with T owing to relativistic effects. However, a different result can arise for a dense quantum medium.

IV. EXAMPLES

A. Hadrons in heavy-ion collisions

1. Production of ρ mesons via the $\rho \leftrightarrow \pi\pi$ process

First, we consider an example of ρ-meson thermal decay and production in a thermal and chemically equilibrated pion bath:

$$\rho^0 \leftrightarrow \pi^+ + \pi^-, \quad (50)$$

$$\rho^\pm \leftrightarrow \pi^\pm + \pi^0. \quad (51)$$

In this example all particles are bosons and we put $m_1 = m_2$ for simplicity, which is not quite exact for reaction (51). In

integral (42) we have $E_1 = E_2 = m_\rho/2$ in the ρ rest frame. The integrand in $\Phi(p)$ is a symmetric function. Then we can write

$$\Phi(p_\rho) = 2\int_0^1 d\zeta \frac{\Upsilon_\pi^{-2}}{\Upsilon_\pi^{-1}e^{(a-b\zeta)}-1}\frac{1}{\Upsilon_\pi^{-1}e^{(a+b\zeta)}-1}, \quad (52)$$

where

$$a = \frac{\sqrt{m_\rho^2+p_\rho^2}}{2T}; \quad b = \frac{\sqrt{1-4m_\pi^2/m_\rho^2}\,p_\rho}{2T}. \quad (53)$$

The integral, Eq. (52), can be evaluated in this case as

$$\Phi(p_\rho) = \frac{2\Upsilon_\pi^{-2}}{b\left(\Upsilon_\pi^{-2}e^{2a}-1\right)} \times \left[b + \ln\left(1+\frac{\Upsilon_\pi(e^{(b-a)}-e^{-(a+b)})}{(1-\Upsilon_\pi e^{b-a})}\right)\right]. \quad (54)$$

Then we substitute Φ into Eq. (39), and using Eq. (28) we can calculate ρ decay and production rates. To calculate $\tau_3 \to \tau$ we use definition (29).

In Fig. 4 we present the ρ decay time in the laboratory frame normalized by its decay time in the rest frame in a vacuum as a function of temperature T for $\Upsilon_\rho = \Upsilon_\pi = 1$ [solid (red) line], $\Upsilon_\rho = \Upsilon_\pi = 2.56$ (dashed line), and $\Upsilon_\rho = \Upsilon_\pi = 0.1$ (dash-dotted line); the dotted line shows the Boltzmann limit, Eq. (49). We consider the range of temperatures between 50 and 150 MeV, which includes the QGP hadronization temperature (≈140–165 MeV).

We show the case $\Upsilon_\rho = \Upsilon_\pi = 0.1$ (dot-dashed line) to check the transition to the Boltzmann limit. We can see that for this case, the result is close to the Boltzmann approximation for our range of T, as expected. In the case of chemical equilibrium, $\Upsilon_\rho = \Upsilon_\pi = 1$, the solid line in Fig. 4 shows a relatively small, 10%–15% increase in life span. We finally consider a supersaturated pion state, $\Upsilon_\rho = \Upsilon_\pi = 2.56$, which can arise after supercooled QGP hadronization near $T = 140$ MeV [8]. For small $T \ll m_\rho/2$, the ratio τ/τ_0 is near the Boltzmann limit, close to unity, because for such a small T, when the Boltzmann limit is applied, the decay time τ does not depend on Υ. When T increases quantum effects dominate and τ decreases with increasing T. In general, the larger Υ is, the more rapidly τ decreases with temperature.

Here we do not consider in depth the ρ-meson density evolution in heavy-ion collisions, because without doubt, our limited system (just a few hadron states) is not sufficiently realistic to capture the physics of the ρ in dense matter. Moreover, the ρ yield is a probe of the hadron density temporal evolution and thus still more difficult to describe precisely. This can be seen as follows: In the Boltzmann low-density limit, the chemical equilibration time is $\tau_\rho \approx 1.7$ fm. Our result shows that the pion high-density quantum medium effects causes an increase in ρ width, that is, a decrease in equilibration time to $\tau_\rho \approx 1.25$ fm, accelerating ρ-meson chemical equilibration near the hadronization temperature. The kinetic-phase time scale in heavy-ion collisions, when hadrons interact, is near 2–3 fm [6]. This means that the ρ-meson chemical evolution is dependent on the ambient hadron density and thus is intricately connected with the dynamics of fireball expansion.

2. ϕ-meson evolution in heavy-ion collisions

We consider here ϕ-meson yield evolution in a thermal hadronic gas after QGP hadronization formed in heavy-ion collisions. The temperature of QGP hadronization can be within the range 140–180 MeV. After hadronization, individual hadrons can continue to rescatter into resonances in what we call the kinetic evolution phase or thermal hadronic gas. This scattering effect does not materially change the final stable particle yields, but it affects the yields of resonances observed by the invariant mass method. The temperature of kinetic-phase freeze-out is expected to be near 100 MeV. After kinetic freeze-out, hadrons expand without interactions, via decay only.

The ϕ meson has, on the hadron reaction scale a relatively small width, $\Gamma_\phi \approx 4.26$ MeV, that is, $\tau_\phi \approx 46$ fm, which is much longer than the duration of the kinetic phase. About 83% of ϕ mesons decay into $K + K$. Therefore we consider here ϕ evolution in the reaction

$$K + K \leftrightarrow \phi. \quad (55)$$

We do not consider here the decay channel $\phi \to \rho + \pi$, which is about 15% and can influence our result at this level. Moreover, the ϕ inelastic scattering in two- to two-particle reactions also has a noticeable influence on ϕ yield, about 15% suppresion [10]. In Ref. [10] only the ϕ decay was included, without the reverse reaction, assuming an initial equilibrium yield at hadronization. We show here how the reverse reaction and nonequilibrium hadronization conditions can influence the resulting ϕ yield. The effect from the full one-to-two reactions, Eq. (55), can be added to that from two-to two-particle reactions.

We did a similar study previously for baryon resonances $\Delta(1232)$ and $\Sigma(1385)$ [6]. We found that in the case of initial nonequilibrium yield, when we have an overabundance of stable particles at hadronization, the resonance production can be greater than the resonance decay. Decay becomes dominant when the temperature drops with expansion, and the lighter-mass decay product state becomes statistically preferable. The final resonance yield depends on the study of the balance between these two effects.

The ϕ-meson width is smaller than the width of these baryon resonances, and its yield change during the posthadronization kinetic phase is expected to be smaller. However, the rather low threshold energy, $m_\phi - m_K - m_K \approx 30$ MeV, could mean that ϕ production is dominant over a longer period of time than in the aforementioned case of baryon resonance. The purpose of this short study is to determine how much the yield of ϕ can change during the kinetic phase owing to kaon fusion compared to its yield at hadronization. We do not study how relativistic and quantum effects influence the reaction, Eq. (55), relaxation time, because for the range of temperature considered these effects are small.

Considering that the mass of all particles involved is greater than the temperature, it is possible to use the Boltzmann

distribution for ϕ and K:

$$\frac{N_\phi}{V} = \Upsilon_\phi \frac{T^3}{2\pi^2} g_\phi x_\phi^2 K_2(x_\phi), \tag{56}$$

$$\frac{N_K}{V} = \Upsilon_K \frac{T^3}{2\pi^2} g_K x_K^2 K_2(x_K), \tag{57}$$

where $x_i = m_i/T$, and $K_2(x)$ is the Bessel function. We proceed as in Ref. [6], using Eq. (31).

Initial conditions in the kinetic phase are defined by conditions at QGP hadronization. We introduce the initial hadron yields in a framework of a rapid QGP hadronization, with all hadrons produced with yields governed by the entropy and strangeness content of QGP by quark recombination. In this model the yields of mesons and baryons are controlled by the constituent quark fugacity γ_q:

$$\Upsilon_K^0 = \gamma_q \gamma_s; \quad \Upsilon_\phi^0 = \gamma_s^2. \tag{58}$$

Thus for $\gamma_q > 1$ we have the condition $\Upsilon_\phi < \Upsilon_K \Upsilon_K$. At first, the reaction goes toward ϕ production until the ϕ density reaches the equilibrium point when the right-hand side of Eq. (31) is 0. If the ϕ density has enough time to reach this point, it begins to decrease again because the temperature decreases owing to expansion.

For each entropy content of the QGP fireball, the corresponding fixed background value of γ_q can be found once the hadronization temperature is known [8]. For $T = 140$ MeV pions form a nearly fully degenerate Bose gas with $\gamma_q \simeq 1.6$. In the following discussion, besides this initial condition, we also consider the value pairs $T = 160$ MeV with $\gamma_q = 1.27$ and $T = 180$ MeV with $\gamma_q = 1$. The value of $\gamma_s \geqslant 1$ plays no significant role as, in the reaction considered, Eq. (55), the number of strange quarks present is the same.

In Fig. 5 we present results for the ratio ϕ/ϕ_0 at different hadronization temperatures as functions of temperature T, beginning from the presumed initial hadronization temperature T_0 through $T_{\min} = 90$ MeV. ϕ^0 is the initial yield obtained at each hadronization temperature. For hadronization

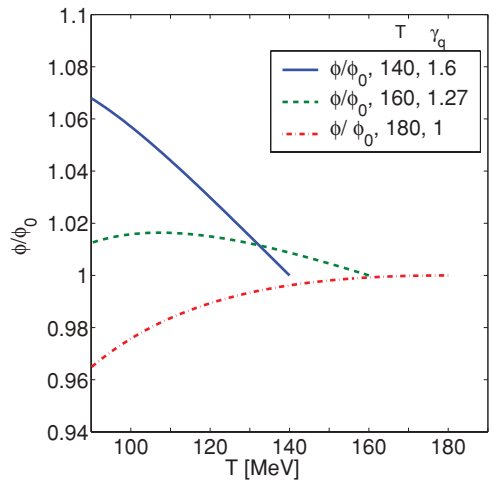

FIG. 5. (Color online) The yield ratio ϕ/ϕ^0 for hadronization temperatures $T_0 = 140$ MeV [solid (blue) line], $T_0 = 160$ MeV [dashed (green) line], and $T_0 = 180$ MeV [dash-dotted (red) line] as functions of the ambient temperature T.

temperature $T_0 < 180$ MeV ($\gamma_q = 1.6$), we initially have $\Upsilon_\phi < \Upsilon_K \Upsilon_K$. In these cases the master equation leads to an initial increase in the yield of resonances. In the case $T_0 = 140$ MeV, when the effect is largest, this increase in ϕ yield continues over the full range of temperature considered. However, the effect is relatively small, about 7%, owing to the small ϕ width. For hadronization temperature $T = 160$ MeV, when $\gamma_q = 1.27$ is smaller, the increase in yield is smaller, and at $T = 105$ MeV the ϕ yield begins to decrease slowly owing to the dynamics of the expansion.

We note that for $T \geqslant 180$ MeV there is always a slow depletion of the ϕ resonance yield. This result implies that the observed yield of ϕ has a systematic $+7\%/-4\%$ uncertainty owing to kaon rescattering in the medium. For comparison, in Ref. [10] the effect from ϕ decay only for an equilibrium yield at hadronization ($\gamma_q = \gamma_s = 1$) was determined to be -7.5% and the effect from two- to two-particle reactions was -15%. Therefore ϕ production in kaon fusion for nonequilibrium hadronization conditions may have an enhancement effect of about 15% on the final ϕ yield, compared to the scenario where the ϕ can only decay after in-equilibrium hadronization formation.

We cannot compare with experimental results considering only the kaon fusion reaction, as it was argued in Ref. [10] that certain two-to-two reactions and possibly other processes can influence the yield. We note only that kaon fusion can add to the observed ϕ yield [11].

B. Freeze-out processes in the early Universe

1. π^0 at $T \ll m_\pi$

As mentioned in Sec. I, it is interesting to examine the mean lifetime of π^0 in the end of the hadronic-gas stage of the Universe where the temperature drops to a mega-electron-volt level in the low teens. Then the reaction

$$\pi^0 \leftrightarrow \gamma + \gamma$$

determines the abundance of π^0.

The difference from the previous example is that the photons are massless and they are always in chemical equilibrium in the early Universe ($\Upsilon_1 = \Upsilon_2 = 1$). Then we can rewrite function (45) as

$$\Phi(p_{\pi^0}) = \frac{2}{b(e^{2a}-1)}\left[b + \ln\left(1 + \frac{e^{(b-a)} - e^{-(a+b)}}{1 - e^{b-a}}\right)\right], \tag{59}$$

with

$$a = \frac{\sqrt{m_{\pi^0}^2 + p_{\pi^0}^2}}{2T}; \quad b = \frac{p_{\pi^0}}{2T}. \tag{60}$$

Again, using Eqs. (39) and (28) we can calculate the π_0 decay and production rates. To calculate τ for π^0 decay in matter, we use definition (29).

In Fig. 6 we show the ratio of the π^0 decay time $\tau_3 \to \tau$ in the presence of thermal particles to the decay time in vacuum in the π_0 rest frame: $\tau_{\pi^0}/\tau_{\pi^0}^0$. In this figure a wider range of temperature is shown: 1–200 MeV. For $\Upsilon_{\pi^0} = 1$ the ratio

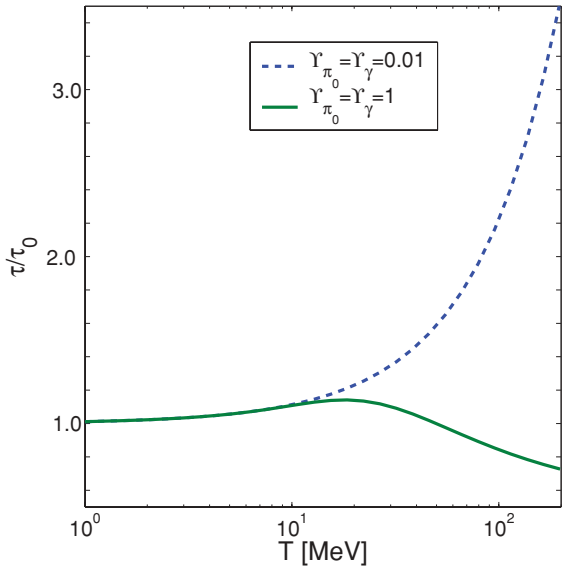

FIG. 6. (Color online) The ratio τ/τ_0 for π^0 decay and production as a function of temperature T. Dashed (blue) line is for a dilute system, $\Upsilon_{\pi^0} = \Upsilon_\gamma = 0.01$ (Boltzmann limit); solid (green) line is for a thermal chemically equilibrated system, $\Upsilon_{\pi^0} = 1$.

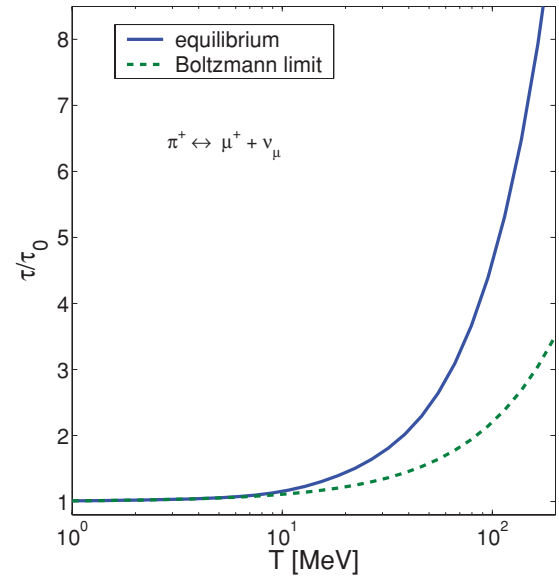

FIG. 7. (Color online) $\pi^\pm$ relaxation time as a function of T in reaction (6), in thermal equilibrium [solid (blue) line], and in the Boltzmann limit, obtained for $\Upsilon = 0.01$ [[dashed (green) line].

$\tau_{\pi^0}/\tau^0_{\pi^0}$, the temperature dependence, is similar to that for ρ decay, considered in the previous section. It increases at first, owing to relativistic time dilution effects. Then, after $T \approx 20$ MeV, τ goes down slowly with temperature, when the quantum in-medium effect becomes important. Quantum in-medium effects arise here mostly from photons. They compensate the relativistic Lorentz factor effect when T is about m_π; compare the lines in Fig. 6 for $\Upsilon_\pi = \Upsilon_\gamma = 0.01$ [dashed (blue) line] and $\Upsilon_\pi = \Upsilon_\gamma = 1$ [solid (green) line]. Note that when the yield of pions is small, that is, only Υ_π is small, the result is almost the same as in chemical equilibrium, $\Upsilon_\pi = \Upsilon_\gamma = 1$.

As long as the π_0 reaction relaxation time τ is much shorter compared to the Hubble expansion time $T/\dot{T} = 1/H$, there is chemical equilibrium in the Universe with $\Upsilon_{\pi^0} = 1$. Freeze-out from chemical equilibrium arises when condition Eq. (36) is satisfied. Because $\tau \approx \tau_0 = 8.4 \times 10^{-17}$ s the condition, Eq. (36), is always satisfied where π^0 can exist. Only at unrealistically high temperatures can this condition be violated.

Therefore we conclude that for the temperature range of interest, between a few and 180 MeV, the π^0 are in chemical equilibrium with photons because of their fast reaction rate. Note that a weak interaction process such as neutron decay $n \to p + e^- + \nu_e$ is 20 orders of magnitude slower, and the Universe expansion rate can dominate the neutron decay rate, for example, at $T > 0.1$ MeV, before having a good chance to decay, neutrons are thus available to enter nuclear reactions.

The pion and muon equilibrium density is high until temperatures near a few mega–electron volts, and as a result, they participate in reactions with each other, nucleons and other particles; for example, see the next sections. The importance of this realization of pion chemical equilibrium in the Universe is that it implies that all hadron species driven by pions also remain in chemical equilibrium. Their abundances can thus be computed using the chemical equilibrium hypothesis, as done in Ref. [4].

2. $\pi^\pm$, $\mu^\pm$, and ν, $\bar{\nu}$ equilibration/freeze-out

In the laboratory the dominant $\pi^\pm$ production reaction is the pion charge exchange reaction, Eq. (5), which we considered in Ref. [3]. These reactions also can take place in the early Universe. However, given the much slower evolution of the early Universe, we also now encounter reactions involving neutrinos, Eq. (6); the related in-vacuum, weak-decay lifespan of the $\pi^\pm$ is $\tau_0 = 2.60 \times 10^{-8}$ s.

In Fig. 7 we show the relaxation times in units of τ_0 for $\pi^\pm$ equilibration, Eq. (29), in reaction (6), as functions of temperature: near $T \simeq 160$ MeV the life span is enhanced by a factor of 3 for thermal equilibrium densities with Υs $= 1$ [solid (blue) line in Fig. 7], mostly owing to Pauli blocking of the decay products. The time dilation owing to thermal motion, which also prolongs the life span, has a smaller effect, visible in the Boltzmann limit, which we study for a dilute system with Υs $= 0.01$ [dashed (green) line].

Interestingly, as we next show, the process, Eq. (6), is the fastest mechanism of neutrino equilibration in a wide range of temperatures relevant here, $T > 7$ MeV, but the ν_μ-freeze-out condition is at a lower T and seems to be controlled by the reaction [12]

$$e^+ + e^- \leftrightarrow \nu_{e,\mu} + \bar{\nu}_{e,\mu}, \tag{61}$$

which we also consider now. The neutrino oscillation effect assures that all neutrinos remain in equilibrium as long as one is strongly coupled to the system.

In Fig. 8 we show the muon-neutrino equilibration time in reaction (6) [solid (blue) line]; recall that to obtain this relaxation time from the results shown in Fig. 7, we need to

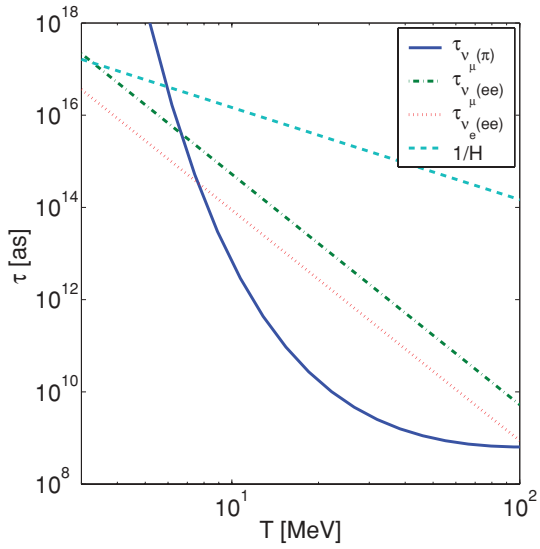

FIG. 8. (Color online) Relaxation time for neutrino ν_μ equilibration as a function of temperature compared to the Universe expansion time $1/H$ [dashed (turquoise) line]. Solid (blue) line represents reaction (6) with equilibrium densities ($\Upsilon = 1$); dash-dotted (green) line and dotted (red) line are for reaction (61) for muon and electron neutrino, respectively.

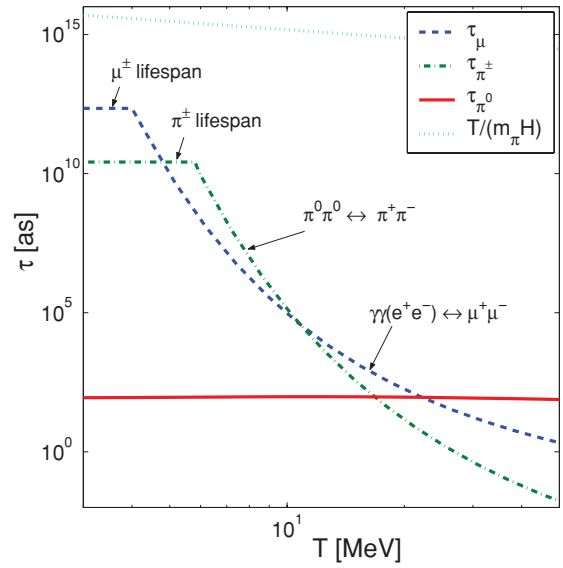

FIG. 9. (Color online) Equilibration times as functions of temperature, for π^0 [solid (red) line], $\pi^\pm$ [dash-dotted (green) line], $\mu^\pm$ [dashed (blue) line], and $\tau_T \approx T/(Hm_\pi)$ [dotted (turquoise) line].

replace the π density in the nominator of Eq. (29) by the density of ν. This relaxation time intersects the Universe expansion rate at $T \approx 5.5$ MeV. Freese *et al.* [12] obtain the relaxation time as a function of T assuming the neutrino chemical potential $\mu_\nu \ll T$ in reaction:

$$\tau_{\nu_\mu(ee)} = (0.1 G_F T^5)^{-1}, \quad \tau_{\nu_e(ee)} = (0.6 G_F T^5)^{-1}, \qquad (62)$$

where $G_F = 1.1664 \times 10^{-5}$ GeV^{-2} is the Fermi constant. These two results are shown in Fig. 8. We see that the muon-neutrino freeze-out temperature according to reaction (6) is slightly higher than that according to reaction (61). The temperature of the neutrino decoupling in reaction is $T_d \cong 3.5$ MeV for ν_μ and $T_d \cong 2.0$ MeV for ν_e.

For a wide range of temperatures, to as low as 7 MeV, neutrino chemical equilibration by reaction (6) is dominant. This example shows that reactions with chemically equilibrated pions and muons can have an influence on other, even lighter particle evolution for temperatures $T \ll m$.

Muons can be equilibrated by reaction (7) and by the $1 \leftrightarrow 3$ reaction [Eq. (8)]. We do not consider this type of reaction in detail here. For low temperatures, $T \ll m_\mu$, when relativistic and medium effects are small, we assume that the muon decay time and reverse reaction relaxation time are nearly the muon life span in vacuum, $\tau_0 = 2.20 \times 10^{-6}$ s.

In Fig. 9 we show relaxation times for dominant reactions for pion and muon equilibration. For the $\pi^\pm$ reaction, Eq. (6), becomes dominant over reaction (5) at $T \approx 6$ MeV. For the $\mu^\pm$ reaction Eq. (8) becomes dominant at $T \approx 4$ MeV. Therefore at these low temperatures, relaxation times for $\mu^\pm$ and $\pi^\pm$ equilibration become constant and far below the Universe expansion rate and τ_T [dotted (turquoise) line]. We conclude that $\mu^\pm$ and $\pi^\pm$ stay in chemical equilibrium. This does not mean that they play an important role in the global physics of the early Universe, because just at these temperatures, muon and pion densities begin to drop rapidly and soon their yield is negligibly small, far below the nucleon density in the Universe.

V. CONCLUSIONS

We have presented details of the kinetic master equation for a process involving the formation of an unstable particle through reaction (11) in a relativistically covariant fashion. Assuming that all particles in the process are in thermal equilibrium, we calculated the thermal averaged decay and formation rates of the unstable particle. Using the time reversal symmetry of quantum processes, we have shown that the time evolution of the density of an unstable particle is given by Eq. (13). Therefore in chemical equilibrium the particle fugacities are connected by Eq. (18). We have explicitly derived the thermal decay rate of an unstable particle, obtaining Eq. (44).

The general properties of the thermal particle decay/production kinetics have led us to consider the relaxation time defined by Eq. (29), which results in a greatly simplified kinetic equation, Eq. (31). The medium modification of reaction rates we encountered are all caused by final-state quantum effects, Bose enhancement, and/or Fermi blocking, absent in the Boltzmann limit. Moreover, we note the presence of kinematic effects, in that all life spans of particles are time dilated owing to their motion with respect to the thermal bath rest frame.

In the present formalism, we assume that the decay width of an unstable particle is much smaller than the temperature T. This approximation is safe in the examples we have discussed, except perhaps the case of ρ decay, where some corrections may be needed. For the formation of heavy resonances, whose decay width becomes appreciable compared to the temperature T, we may need to include the finite-width effect on the mass

of an unstable particle in the thermal distribution. Such effects on the statistical partition function and the equation of state of a system have been studied based on the virial expansion method [13]. The correction for a kinetic equation in such a case has also been studied [14].

We have presented several examples, $\rho \leftrightarrow \pi + \pi$, $\phi \leftrightarrow K + \overline{K}$, $\pi^0 \leftrightarrow \gamma + \gamma$, and $\pi^\pm \leftrightarrow \mu^\pm + \nu_\mu(\bar{\nu}_\mu)$, and explored the physics cases of hot hadron matter created in laboratory heavy-ion reactions and the early Universe from the condition of hadronization down to the temperature of several mega–electron volts. The two first processes can take place in both circumstances. The third process is important to the understanding of how the hadronic fraction evolves with the expansion of the Universe. The last process we considered appears to be the dominant mechanism of neutrino equilibration over the entire temperature range, except close to neutrino freeze-out, a result that requires further refinement allowing for finite chemical potentials. This example also shows that heavy ($m \gg T$) chemically equilibrated particles can be important in the evolution of other particles, including lighter more dense particles yields at relatively low temperatures.

The equilibration-relaxation time for π^0 decay remains close (within 25%) to the relaxation time in vacuum over a large temperature range. This occurs because the relativistic effect (Lorentz factor) is compensated by the quantum medium effect. This time is short compared to the Universe expansion time for all temperatures of interest here, below the GQP hadronization temperature, when π^0 hadrons are created. Therefore π^0 always stays in chemical equilibrium with radiation for the temperature range of interest.

As long as π^0 is abundant it can participate in reactions with other hadrons and influence the dynamics of the Universe evolution. Here we also considered $\pi^\pm$ evolution, in the fourth reaction given, and their interaction with π^0. We showed that pions and muons (mesons) stay in chemical equilibrium throughout the evolution of the Universe, despite their large mass. They can be involved in reactions with nucleons, a topic we postpone to a future study, down to temperatures where the meson density drops well below the nucleon density. The contribution of mesons disappears from the entropy and the degeneracy g only at the relatively low $T \approx 10$ MeV (see Fig. 3).

Our study of the ϕ evolution in thermal hadron medium after GQP hadronization in heavy-ion collisions, suggests a possible slight modification of the observed ϕ yield: compared to initial production, an increase in hadronization at $T = 140$ MeV, $\gamma_q = 1.6$, at the level of about 6%–7%, or a suppression of about 4% for hadronization at $T = 180$ MeV, $\gamma_q = 1$.

To conclude, we have presented here the process of decay and re-creation of unstable particles and studied special cases of relevance to heavy-ion collisions and the early Universe. Our results indicate that the early Universe was in chemical equilibrium throughout its evolution and that the first freeze-out occurs when neutrinos decouple.

ACKNOWLEDGMENTS

We thank H. Th. Elze, M. J. Fromerth, T. Kodama, J. Letessier, M. Makler, and R. L. Thews for valuable discussions regarding hadron-phase chemical equilibration in the early Universe. We thank T. Kodama for contributing, 9 years ago, an unpublished private communication about the method and essential results regarding π^0 equilibration using the detailed balance method and for close reading of the manuscript and valuable comments. This work was supported by US Department of Energy Grant No. DE-FG02-04ER41318.

[1] See, e.g., J. Bernstein, *Kinetic Theory in the Expanding Universe* (Cambridge University Press, Cambridge, 1988), ISBN-10:0521360501; D. D. Clayton, *Principles of Stellar Evolution and Nucleosynthesis* (McGraw-Hill Education, New York, 1968).

[2] E. W. Kolb and M. S. Turner, *The Early Universe* (Perseus Books Group, New York, 1993).

[3] I. Kuznetsova, D. Habs, and J. Rafelski, Phys. Rev. D **78**, 014027 (2008)

[4] M. J. Fromerth and J. Rafelski, arXiv:astro-ph/0211346; line in figure from J. Rafelski and M. Fromerth, lecture, Landek Zdroj Winter School, Febrary 2–12, 2003; available at [http://www.physics.arizona.edu/rafelski/PS/LandekUniv031.pdf].

[5] J. Letessier and J. Rafelski, *Hadrons and Quark-Gluon Plasma* (Cambridge University Press, Cambridge, 2005).

[6] I. Kuznetsova and J. Rafelski, Phys. Lett. B **668**, 105 (2008).

[7] I. Kuznetsova and J. Rafelski, Phys. Rev. C **79**, 014903 (2009).

[8] I. Kuznetsova and J. Rafelski, Eur. Phys. J. C **51**, 113 (2007).

[9] E. A. Uehling and G. E. Uhlenbeck, Phys. Rev. **43**, 552 (1933); see also L. P. Kadanoff and G. Baym, *Quantum Statistical Mechanics* (Benjamin, New York, 1962).

[10] L. Alvarez-Ruso and V. Koch, J. Phys. G **28**, 1527 (2002); Phys. Rev. C **65**, 054901 (2002).

[11] B. I. Abelev *et al.* (STAR Collaboration), Phys. Rev. C **79**, 064903 (2009).

[12] K. Freese, E. W. Kolb, and M. S. Turner, Phys. Rev. D **27**, 1689 (1983).

[13] G. E. Beth and E. Uhlenbeck, Physica **4**, 915 (1937); for relativistic generalization, see R. Dashen, S. Ma, and H. Bernstein, Phys. Rev. **187**, 345 (1969).

[14] F. Laloe and W. J. Mullin, J. Stat. Phys. **59**, 725 (1990); K. Morawetz and G. Roepke, Phys. Rev. E **51**, 4246 (1995).